

Accepted Manuscript

Design and synthesis of *cis*-restricted benzimidazole and benzothiazole mimics of combretastatin A-4 as antimitotic agents with apoptosis inducing ability

Md. Ashraf, Thokhir B. Shaik, M. Shaheer Malik, Riyaz Syed, Prema L. Mallipeddi, M.V.P.S. Vishnu Vardhan, Ahmed Kamal

PII: S0960-894X(16)30655-2

DOI: <http://dx.doi.org/10.1016/j.bmcl.2016.06.044>

Reference: BMCL 23997

To appear in: *Bioorganic & Medicinal Chemistry Letters*

Received Date: 15 April 2016

Revised Date: 14 June 2016

Accepted Date: 16 June 2016



Please cite this article as: Ashraf, Md., Shaik, T.B., Shaheer Malik, M., Syed, R., Mallipeddi, P.L., Vishnu Vardhan, M.V.P.S., Kamal, A., Design and synthesis of *cis*-restricted benzimidazole and benzothiazole mimics of combretastatin A-4 as antimitotic agents with apoptosis inducing ability, *Bioorganic & Medicinal Chemistry Letters* (2016), doi: <http://dx.doi.org/10.1016/j.bmcl.2016.06.044>

This is a PDF file of an unedited manuscript that has been accepted for publication. As a service to our customers we are providing this early version of the manuscript. The manuscript will undergo copyediting, typesetting, and review of the resulting proof before it is published in its final form. Please note that during the production process errors may be discovered which could affect the content, and all legal disclaimers that apply to the journal pertain.

Design and synthesis of *cis*-restricted benzimidazole and benzothiazole mimics of combretastatin A-4 as antimitotic agents with apoptosis inducing ability

Md. Ashraf,^a Thokhir B Shaik,^{ac} M Shaheer Malik,^a Riyaz Syed,^a Prema L.Mallipeddi,^b M V P S Vishnu Vardhan,^a Ahmed Kamal,^{*a}

^a*Medicinal Chemistry and Pharmacology, CSIR-Indian Institute of Chemical Technology, Tarnaka, Hyderabad 500 007, India*

^b*GVK Biosciences Pvt. Ltd., Plot No 79, IDA, Mallapur, Hyderabad 500076, Andhra Pradesh, India.*

^c*Acharya Nagarjuna University, Nagarjuna Nagar, Guntur 522510, India.*

Key words: Tubulin inhibitor, combretastatin A-4, benzimidazole, benzothiazole, apoptosis.

Abstract: A series of colchicine site binding tubulin inhibitors were designed and synthesized by the modification of the combretastatin A-4 (CA4) pharmacophore. The ring B was replaced by the pharmacologically relevant benzimidazole or benzothiazole scaffolds, and the *cis*-configuration of the olefinic bond was restricted by the incorporation of a pyridine ring which is envisaged by the structural resemblance to a tubulin inhibitor like E7010. These compounds were evaluated for their antiproliferative activity on selected cancer cell lines and an insight in the structure activity relationship was developed. The most potent compounds (**6c** and **6l**) demonstrated an antiproliferative effect comparable and superior to that of CA4 (GI₅₀ up to 40 nM). Mitotic cell cycle arrest in G2/M phase revealed the disruption of microtubule dynamics that was confirmed by tubulin polymerization assays and immunocytochemistry studies at the cellular level. The molecular docking studies suggested that the binding of these mimics at the colchicine site of the tubulin is similar to that of combretastatin A-4.

Introduction:

Microtubules are one of the key structural components of the cytoskeleton in eukaryotic cells comprising of α and β -tubulin heterodimers. They play a crucial role in various cellular processes

and have emerged as an attractive and viable target in the development of anticancer drugs mainly due to their indispensability in mitotic cell division.¹ Generally, drugs that target microtubules bind to one of three main sites of tubulin,² which includes the paclitaxel site for the microtubule stabilizing agents,^{3,4} the *vinca* domain⁵ and the colchicine domain^{6,7} for the destabilizing agents. Interfering with the dynamic stability of microtubules, these agents acts as spindle poisons arresting the dividing cells in G2/M phase of the cell cycle, causing mitotic catastrophe and finally leading to apoptotic cell death. Some of the well-known naturally occurring tubulin binding ligands that affect the microtubule dynamics by binding to distinct colchicine domain of tubulin are colchicines and combretastatin A-4 (Figure 1).^{8,9}

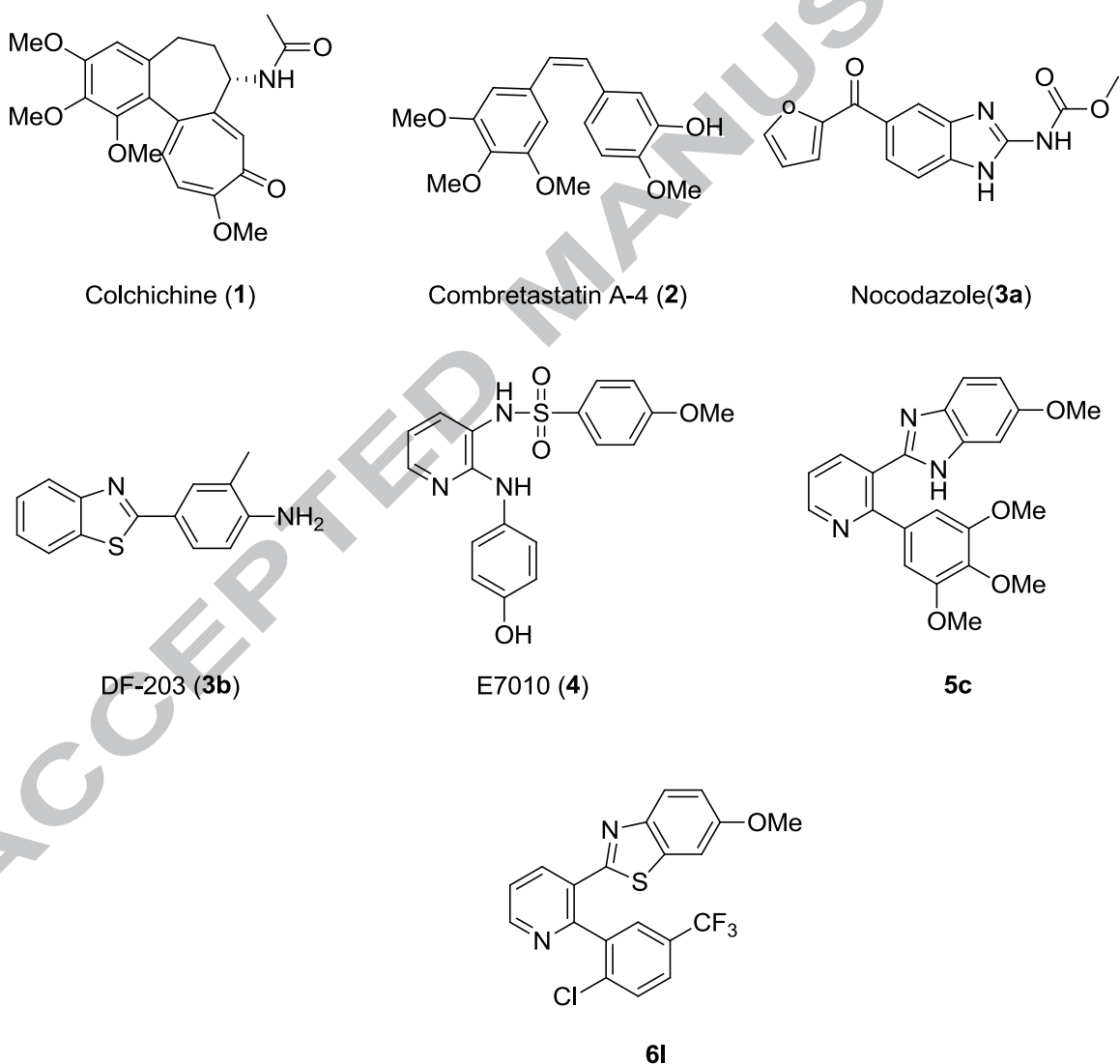


Figure 1. Colchicine site binding microtubule inhibitors

Combrestatin, the *cis* stilbene derivative, isolated from the bark of the South African tree *Combretum caffrum* is one of the simplest and promising molecules among the structurally diverse microtubule perturbing agents. Combretastatin A-4 exhibits remarkably strong inhibition of tubulin polymerization by binding to the colchicine site as well as potent cytotoxicity against murine lymphocytic leukemia, human ovarian and colon cancer cell lines resulting in vascular shutdown in solid tumor.¹⁰⁻¹⁴ In recent years CA4 emerged as a preferred lead compound in the development of new inhibitors of tubulin polymerization because of its high potency and ease of synthesis.^{15,16} Similar to other colchicine site binders, CA4 has three important pharmacophoric substructures, the two hydrophobic rings (A and B) and the linking olefinic bridge with appropriate dihedral angle resulting from the *cis* configuration. It was previously postulated that the presence of trimethoxy substitution on ring A is crucial for efficient binding at colchicine site.⁸ However, of late this substitution pattern on ring A is considered to be not as indispensable as previously assumed.¹⁰ On the other hand, the ring B was found to be tolerant to structural modification and a number of reports defined this ranging from substituted phenyl ring to heterocyclic and nonsubstituted aromatic rings.^{10,17} Importantly, the olefinic bond with *cis* configuration plays a fundamental role in binding at the colchicine site by positioning the rings at appropriate distance to maximize interactions.¹⁸ Several attempts have been reported to modify this *cis*-olefinic bond to prevent its isomerisation under amenable conditions. This mostly included either modification of the olefinic bond by the introduction of saturation, substituents and other functionalities or its replacement with a three to six membered ring system, which resulted in *cis* restricted analogues of CA4.^{16,19-22}

Similar to CA4, a number of colchicine site binding ligands are known to inhibit tubulin polymerization and are considered as potential lead like molecules. One of them, E7010 is the first orally active antimitotic sulphonamide derivative that has received much interest in recent years and currently it is in clinical trials.²³ It binds reversibly to colchicine site of β -tubulin and inhibits tubulin polymerization resulting in cell cycle arrest in M phase. Structure-activity relationship studies of E7010 suggested that the replacement of pyridine moiety and the methoxy as well as hydroxy groups resulted in lowered in vitro and in vivo activity.²⁴⁻²⁶ Research efforts have been directed towards the development analogues of E7010 as inhibitors of tubulin polymerization in cancer drug discovery programs.²⁷⁻²⁸

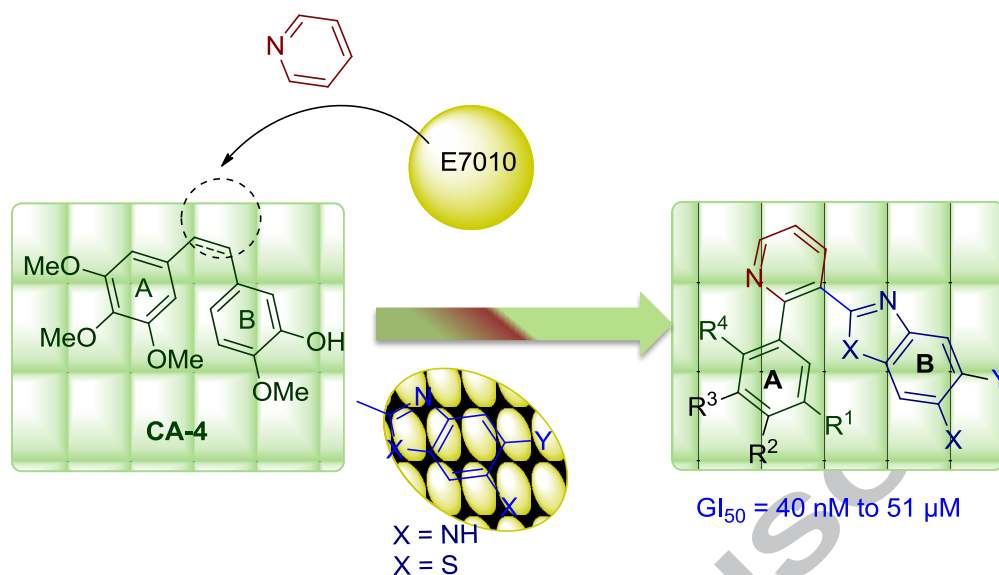
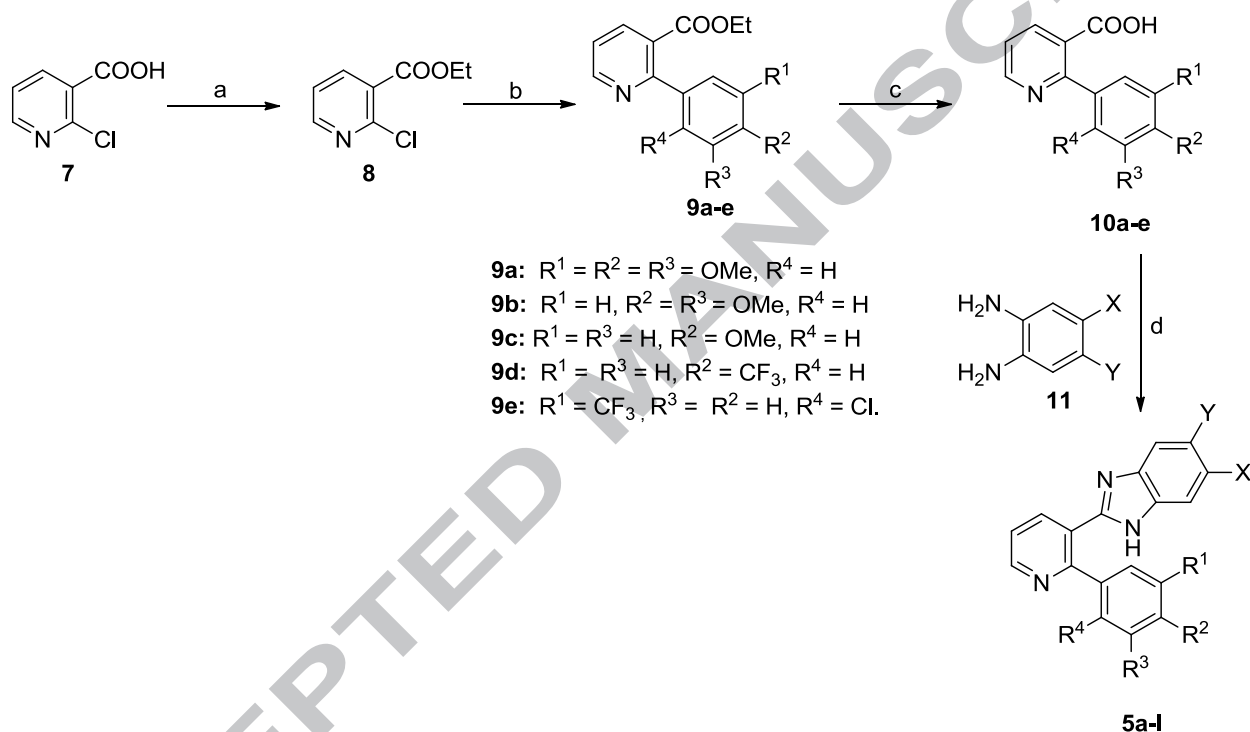


Figure 2. Designing of combretastatin conjugates

Our recent research studies have been mainly focused on the synthesis, evaluation and mechanistic aspects of newer molecules based on different heterocyclic scaffolds as potential anticancer agents.^{29,30} In particular, the targeting of tubulin polymerization by new diversified ligands based on CA4 and E7010 have led to promising and interesting results.³¹ Herein, we describe different modifications on CA4 scaffold, specifically the incorporation of benzimidazole and benzothiazole moieties of pharmacological relevance by replacement of ring B. The rationale behind this is the significance of these moieties as privileged structures and the opportunity offered by them as anchors that could be harnessed for further diversification, besides they are present in number of antimitotic agents such as nocodazole and DF-203.^{32,33} Moreover, the structural resemblance to E7010, a colchicine site binder (with crucial pyridine ring) was envisaged by the replacement of the olefinic bond by a pyridine ring to maintain the *cis* configuration. Such replacements of the olefinic bond with a ring system have been reported to provide potential advantage of promoting tubulin binding activity and tumor selectivity besides minimizing toxicity.¹⁰ In addition, since the constitutive role of the trimethoxybenzene moiety (ring A) is ambiguous in tubulin binding, we modified it with different substitution patterns. The resulting *cis*-restricted benzimidazole and benzothiazole mimics of CA4 were evaluated for antiproliferative activity and examined for their structure activity relationship (SAR) followed by studies to elucidate the mechanism of action which included cell cycle progression, tubulin polymerization assay and molecular docking studies. Further to confirm the induction of

apoptotic cell death by the potent mimics like **6c** and **6l**, studies such as caspase activation, mitochondrial membrane potential.

The synthesis of benzimidazole and benzothiazole mimics of CA4 (**5a-l** and **6a-n**) was accomplished by the synthetic route illustrated in Schemes 1 and 2. In the synthetic route 2-chloronicotinic acid (**7**) was employed as the starting material, which was converted to its ester derivative, ethyl 2-chloronicotinate (**8**) by using sulphuric acid and ethanol in quantitatively yield³¹ (Scheme 1).



Scheme 1. Synthesis of benzimidazole mimics of CA4 (**5a-l**). Reagents and conditions: (a) H_2SO_4 , ethanol, 80°C , 2 h. (b) ArB(OH)_2 , $\text{Pd(PPh}_3)_4$, Na_2CO_3 , toluene-EtOH-water, 120°C , 8 h. (c) 2N NaOH, 1N HCl, ethanol, 80°C , 4 h. (d) polyphosphoric acid, 180°C , 2 h.

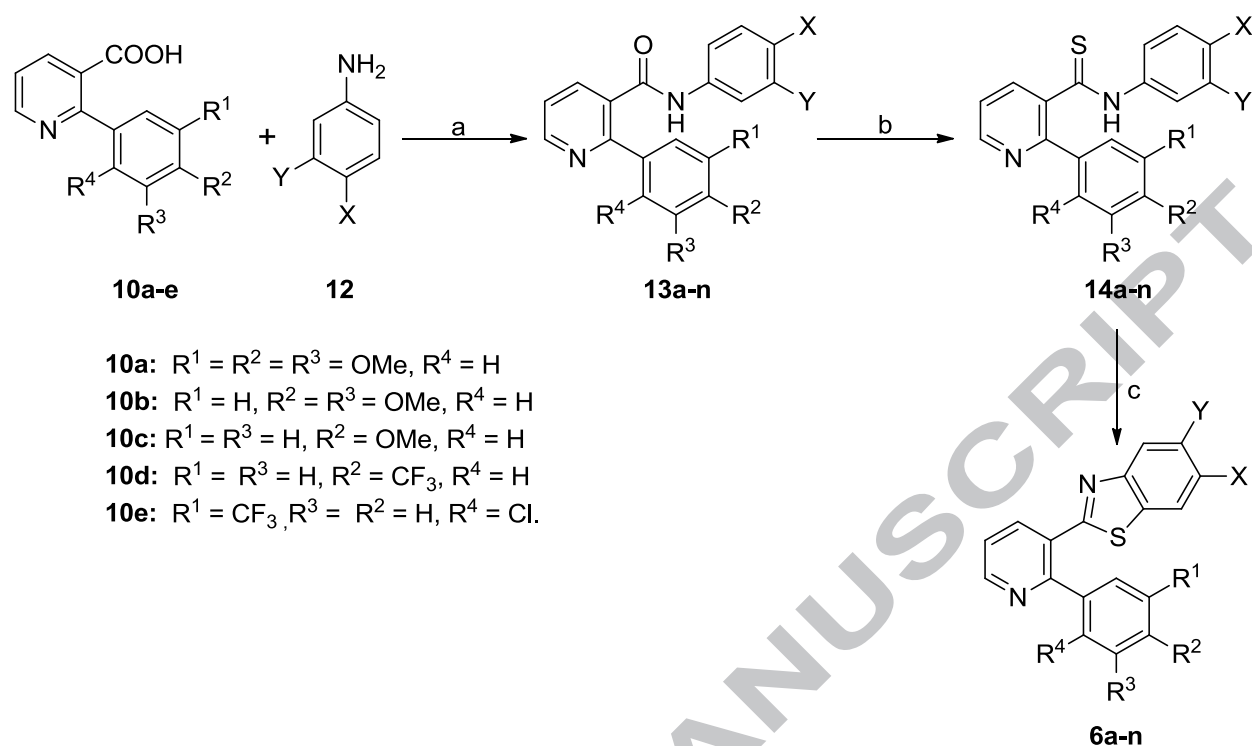
The ester **8** was subjected to Suzuki coupling by condensation with a variety of substituted boronic acids in the presence of tetrakis(triphenylphosphine)palladium and potassium carbonate in toluene and ethanol-water to afford the intermediates **9a-e**, which on subsequent hydrolysis with 2N NaOH solution in ethanol provided 2-phenyl substituted nicotinic acids **10a-e**.³⁴ These key intermediates were utilized in the synthesis of the benzimidazole and benzothiazole mimics

of CA4. These intermediates **10a-e** were condensed with various substituted o-diaminobenzenes (**11**) in the presence of polyphosphoric acid under refluxing condition to afford the desired *cis*-restricted benzimidazole mimics of CA4 (**5a-l**).

Table 1. Percentage of yields of compounds **5a-l**

Comp	R ¹	R ²	R ³	R ⁴	X	Y	Yield (%)
5a	OMe	OMe	OMe	H	OMe	OMe	51
5b	OMe	OMe	OMe	H	H	H	58
5c	OMe	OMe	OMe	H	OMe	H	44
5d	H	OMe	OMe	H	OMe	OMe	60
5e	H	OMe	OMe	H	H	H	56
5f	H	OMe	OMe	H	OMe	H	67
5g	H	OMe	H	H	OMe	OMe	48
5h	H	OMe	H	H	OMe	H	50
5i	H	OMe	H	H	Cl	H	58
5j	H	CF ₃	H	H	OMe	H	46
5k	H	CF ₃	H	H	Cl	H	63
5l	CF ₃	H	H	Cl	OMe	H	60

To access the benzothiazole mimics of CA4, the same intermediates **10a-e** were employed as depicted in Scheme 2. An amide linkage was established by condensation of substituted nicotinic acids (**10a-e**) with a variety of substituted anilines **12** to yield nicotinamide derivatives (**13a-n**) by employing 1-ethyl-3-(3-dimethylaminopropyl)carbodiimide and 1H-benzo[d][1,2,3]triazol-1-ol in *N,N*-dimethylformamide.³⁴ This was followed by the conversion of carbonyl functionality to its analogous of thiocarbonyl group employing Lawessons reagent under refluxing in toluene to provide thioamides **14a-n**. Finally, the intramolecular cyclization was performed by using a standard method of potassium ferricyanide in presence of 10% NaOH solution furnishing the desired *cis*-restricted benzothiazole mimics of CA4 (**6a-n**).³⁵



Scheme 2. Synthesis of benzothiazole mimics of CA4 (**6a-n**). Reagents and conditions: (a) EDCI.HCl, HOBT, DMF, rt. (b) Lawessons reagent, toluene, 100 °C, 3 h. (c) $\text{K}_3[\text{Fe}(\text{CN})_6]$, 10% NaOH, 100 °C, 2 h.

Table 2. Percentage of yields of compounds **6a-n**

Comp	R^1	R^2	R^3	R^4	X	Y	Yield (%)
6a	OMe	OMe	OMe	H	OMe	OMe	41
6b	OMe	OMe	OMe	H	H	H	48
6c	OMe	OMe	OMe	H	OMe	H	45
6d	H	OMe	OMe	H	OMe	OMe	50
6e	H	OMe	OMe	H	H	H	38
6f	H	OMe	OMe	H	OMe	H	46
6g	H	OMe	H	H	OMe	OMe	55
6h	H	OMe	H	H	OMe	H	56
6i	H	OMe	H	H	Cl	H	51
6j	H	CF_3	H	H	OMe	H	55

6k	H	CF ₃	H	H	Cl	H	40
6l	CF ₃	H	H	Cl	OMe	H	46
6m	CF ₃	H	H	Cl	Cl	H	30
6n	CF ₃	H	H	Cl	H	H	42

Initially we evaluated the antiproliferative activity of the compounds **5a-h** against selected human cancer cell lines *viz.*, cervix (HeLa), liver (HepG2), lung adenocarcinoma (A549) and prostate (DU-145), using SRB assay.³⁶ The results of growth inhibitory activities (GI₅₀ values) are shown in micromolar concentrations and CA4 was used as the reference compound (Table 3). Most of the compounds from these series displayed potent broad spectrum growth inhibitory activities against all the tested cancer cell lines. In the SAR studies it was considered to investigate whether the presence of 3,4,5-trimethoxyphenyl substitution influences the activity along with other substituents on the benzimidazole ring. It was observed that the compounds (**5a-c**) containing trimethoxy substitution on ring-A showed relatively strong inhibitory effect than the 3,4-dimethoxy and 4-methoxy substitution with GI₅₀ values in the range of 0.29-14.6 μ M against some representative cancer cell lines. Among them, compound **5c** with a methoxy group on C-6 position of the benzimidazole moiety exhibited promising activity with a GI₅₀ value of 0.29 μ M against prostate cancer cell line. On the replacement of trimethoxy substituted ring A with di and monomethoxy substituted phenyl ring resulted in moderate activity and compound **5d** was the most potent among them exhibiting GI₅₀ value of 1.9 μ M in the liver cancer cell line. The substitution effect on ring A by these studies reaffirmed the importance of 3,4,5-trimethoxy substitution on the cytotoxic effect by these CA4 mimics. We then proceeded to explore the influence of electron withdrawing group on ring A and benzimidazole moiety with respect to the antiproliferative activity. Compounds having electron withdrawing substituents like trifluoromethyl on ring A (**5j-k**) with a methoxy and chloro group on C-6 position of benzimidazole moiety exhibited significant decrease in activity compared to **5c**. Surprisingly when two electron withdrawing substituents were incorporated on the ring A, a substantial increase in the cytotoxic potency was observed. Compound **5l** with trifluoromethyl on C-5 and chloro on C-2 position of ring A and methoxy group on C-6 position of benzimidazole moiety was the most active benzimidazole mimic of CA4 exhibiting an GI₅₀ range of 0.15-0.76 μ M against certain cancer cell lines.

In the benzothiazole counterparts (**6a-h**), in which one of the nitrogen of the benzimidazole moiety was replaced by sulphur, a substantial enhancement in the antiproliferative activity was observed with GI_{50} values in sub-micromolar concentrations against some of the cancer cell lines tested. Similar to benzimidazole mimics, we initially examined the effect of 3,4,5-trimethoxy substitution on ring A with methoxy substituent on C-5 and C-6 position of benzothiazolyl ring. An identical pattern of activity was observed with trimethoxy substitution on ring A exerting relatively stronger influence on activity than di and monomethoxy substitutions. Compound **6c** with trimethoxy groups on ring A and a methoxy substitution on C-6 position of benzothiazole moiety was one of the most potent mimic exhibiting GI_{50} of 0.06 μ M against HeLa liver cancer cell line. On replacement of 3,4,5-trimethoxyphenyl ring with 3,4-dimethoxy and 4-methoxy phenyl ring, the compounds (**6d-i**) exhibited lower growth inhibition against all the tested cell lines, however **6e** displayed promising activity with $GI_{50} < 1$ μ M against HepG2 and A549 cancer cell lines. In the mimics (**6j-k**) with one electron withdrawing substituent, decreased antiproliferative potency was exhibited similar to benzimidazole counterparts. Nanomolar activity was observed in case of **6l** with two electron withdrawing groups on C-2 and C-5 positions of ring A and methoxy group on benzothiazole moiety against all the tested cancer cell lines with GI_{50} ranging from 0.04-0.09 μ M. Interestingly, mimic **6l** exhibited remarkable and superior antiproliferative activity compared to the standard CA4 particularly against HeLa and DU-145 cancer cell lines and were significantly more potent than sulphonamide E7010.

In order to understand that the effect exerted by the two electron withdrawing groups, that is CF_3 at C-5 and Cl on C-2 on ring A towards the antiproliferative activity. We synthesized and examined some mimics (**6m-n**) in this series. Compound **6m** with chloro group on C-6 position of the benzothiazole ring displayed good activity ($GI_{50} < 1.5$ μ M in two cancer cell lines) whereas the absence of substitution in **6n** lowered the antiproliferative activity. Overall, SAR studies of these *cis*-restricted mimics of CA4 suggested the superiority of 3,4,5-trimethoxy substitution compared to the 3,4-dimethoxy and 4-methoxy substitution on ring A which are in agreement with some similar studies on CA4 analogues described in earlier reports.⁸ The introduction of single electron withdrawing group on ring A decreased the antiproliferative activity, however when two electron withdrawing groups were incorporated at C-2 and C-5 position, a remarkable enhancement in the activity was observed. This is when a methoxy substituent is present on C-6

position of the benzimidazole or benzothiazole moiety, which is considered crucial for imparting potent antiproliferative properties.

Table 3. Growth Inhibition values of compounds **5a-l** and **6a-n** on HeLa, HepG2, A549 and DU-145 cancer cell lines.

Compound	GI ₅₀ μ M			
	HeLa ^a	HepG2 ^b	A549 ^c	DU-145 ^d
5a	1.7 \pm 0.22	1.5 \pm 0.14	2.5 \pm 0.19	0.6 \pm 0.14
5b	2.6 \pm 0.24	3.5 \pm 0.15	4.5 \pm 0.19	14.6 \pm 0.24
5c	5 \pm 0.54	0.84 \pm 0.01	1.5 \pm 0.21	0.29 \pm 0.12
5d	7.7 \pm 0.11	1.9 \pm 0.26	7.9 \pm 0.17	4.19 \pm 0.41
5e	- ^e	12.4 \pm 0.32	- ^e	5.8 \pm 0.33
5f	16.6 \pm 0.41	44.8 \pm 0.17	27.6 \pm 0.54	12.0 \pm 0.16
5g	21.4 \pm 0.09	42.5 \pm 0.41	19.5 \pm 0.19	- ^e
5h	31.1 \pm 0.09	- ^e	21.5 \pm 0.25	19.6 \pm 0.09
5i	- ^e	24.5 \pm 0.15	- ^e	34.7 \pm 0.17
5j	- ^e	- ^e	38.2 \pm 0.12	32.1 \pm 0.09
5k	15.8 \pm 0.16	- ^e	18.4 \pm 0.33	- ^e
5l	0.15 \pm 0.01	0.76 \pm 0.01	0.75 \pm 0.02	0.21 \pm 0.01
6a	1.6 \pm 0.02	0.5 \pm 0.01	0.5 \pm 0.01	0.6 \pm 0.04
6b	4.8 \pm 0.19	3.5 \pm 0.21	3.2 \pm 0.26	4.1 \pm 0.11
6c	0.06 \pm 0.001	0.26 \pm 0.02	0.13 \pm 0.01	0.18 \pm 0.03
6d	13.5 \pm 0.11	1.2 \pm 0.62	7.58 \pm 0.32	5.91 \pm 0.16
6e	1.8 \pm 0.22	0.7 \pm 0.14	0.2 \pm 0.19	3.6 \pm 0.24
6f	6.2 \pm 0.14	2.2 \pm 0.21	1.7 \pm 0.11	6.8 \pm 0.32
6g	11.3 \pm 0.11	30.9 \pm 0.14	59.1	- ^e
6h	8.1 \pm 0.17	- ^e	13.3 \pm 0.09	- ^e
6i	7.7 \pm 0.14	3.9 \pm 0.26	7.9 \pm 0.17	0.19 \pm 0.41
6j	15.7 \pm 0.12	- ^e	17.0 \pm 0.16	- ^e
6k	20.4 \pm 0.09	32.5 \pm 0.41	19.5 \pm 0.19	- ^e

6l	0.04 ± 0.001	0.079 ± 0.001	0.091 ± 0.002	0.052 ± 0.001
6m	5.8 ± 0.12	1.2 ± 0.16	1.5 ± 0.16	- ^e
6n	4.89	15.0	7.41	5.49
CA4	0.06 ± 0.002	0.08 ± 0.002	0.06 ± 0.003	0.07 ± 0.003
E7010	4.8 ± 0.22	2.8 ± 0.22	1.8 ± 0.22	1.2 ± 0.3

^aHuman Cervical cancer; ^bLiver cancer; ^cNon-Small Cell Lung Cancer, ^dProstate cancer, ^eGI₅₀ value not attained at the concentration used in the assay.

Mechanistic studies were performed to understand the mode of action of these CA4 based mimics and the most potent compounds (**6c** and **6l**) were selected for further biological investigations. Initially, cell cycle analysis was performed using the cell permeable DNA binding dye propidium iodide to determine whether the antiproliferative effect resulted from cell cycle arrest. For this purpose, HeLa cells were treated with **6c** and **6l** at concentrations of 40 nM as well as 60 nM for 48 h to study the distribution of cells at different phases of cell cycle. The results demonstrated that compared to untreated cells, the cells treated with **6c** and **6l** displayed significant arrest in G2/M phase, the arrest is not only comparable but superior to CA4, particularly at 60 nM concentration (Figure 3). Compounds **6c** and **6l** arrested 40.8% and 54.05% cells, respectively, in G2/M phase compared to 41.48% blocked by CA4. These results demonstrate that the growth inhibitory effects of the CA4 mimics (**6c** and **6l**) are induced because of the arrest in G2/M phase during cell cycle progression in a concentration dependent manner.

Table 4. The percentage of cells in G2/M phase of cell cycle was quantified by flow cytometry.

Compound	G0	G1	S	G2/M
control	5.64	73.28	3.52	17.56
6c -40nm	13.27	51.22	11.86	23.65
6c -60nm	25.35	19.54	14.30	40.80
6l -40nm	8.13	43.00	24.62	24.26
6l -60nm	20.47	15.19	10.30	54.05
CA4-40nm	25.87	17.92	17.34	38.87
CA4-60nm	24.78	17.29	16.44	41.48

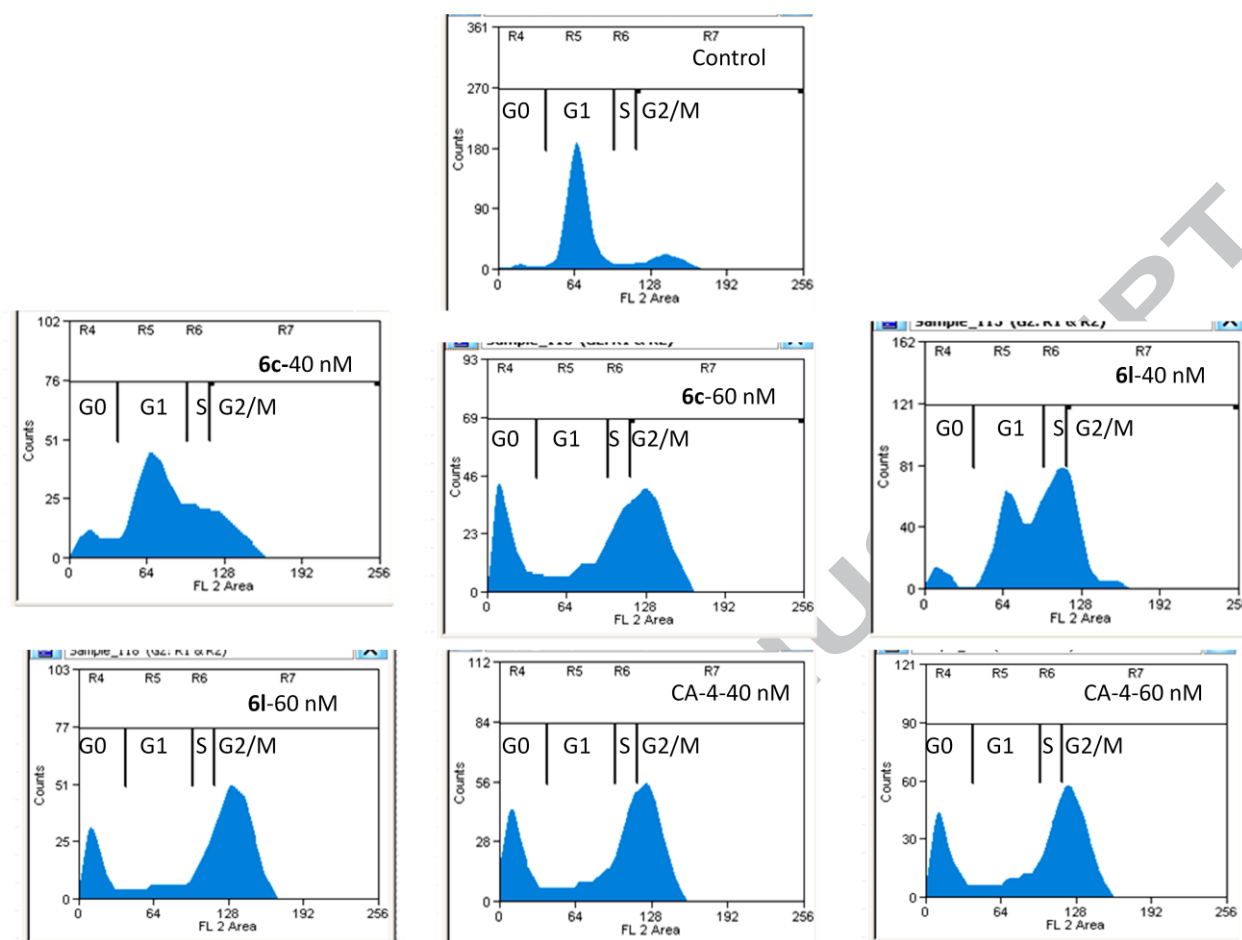


Figure 3. FACS analysis of cell cycle distribution of HeLa cells after treatment with **6c** and **6l** at 40 nM and 60 nM concentrations and CA4 for 48 h. Cell cycle analysis was performed employing propidium iodide as indicated under materials and methods. The percentage of cells in each phase of cell cycle was quantified by flowcytometry.

The G2/M phase arrest of cells takes place due to the perturbation in the mitosis cell division machinery and the tubulin is one of the important structural proteins in the mitosis process. Therefore, as **6c** and **6l** showed significant antiproliferative activity as well as arrest in the G2/M phase in the cell cycle analysis, it is likely that they would inhibit the polymerization of tubulin. The progression in tubulin polymerization was investigated by monitoring the increase in fluorescence emission at 420 nm at 3 μ M concentration employing CA4 as the positive control. These conjugates showed significant activity to inhibit the tubulin polymerization which is comparable to CA4, whereas **6c** inhibited the tubulin polymerization by 60.1% while **6l** inhibited by 68.3% (Figure. 4). The IC₅₀ values of **6c**, **6l** and CA4 are 2.01 ± 0.2 μ M, 1.91 ± 0.23 μ M and 1.87 ± 0.01 μ M respectively (Table 5).

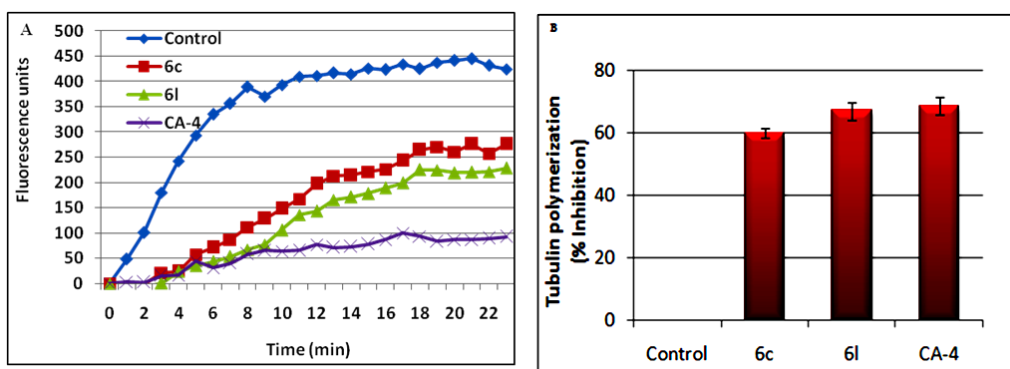


Figure 4. Effect of compounds on tubulin polymerization: Tubulin polymerization was monitored by the increase in fluorescence at 360 nm (excitation) and 420 nm (emission) for 1 h at 37 °C. Synthesized compounds **6c** and **6l** were included at a final concentration of 1 μ M. CA4 was used as a positive control. A) Real time kinetic graph of tubulin polymerization: compounds **6c** and **6l** and CA4 at 1 μ M concentration. B) Percentage of tubulin polymerization inhibition compared to control.

Table 5. IC₅₀ concentration of tubulin polymerization inhibition by mimics **6c**, **6l** and CA4.

Compounds	Tubulin assembly IC ₅₀ \pm SD (μ M)
6c	2.01 \pm 0.2
6l	1.91 \pm 0.23
CA4	1.87 \pm 0.01

To validate the effect of these compounds on the disruption of microtubule dynamics in living cells, studies were carried out to examine the *in situ* effects of **6c** and **6l** on cellular microtubules. HeLa cells seeded on sterile cover slips were treated with these compounds and CA4 was employed as a standard at a concentration of 60 nM for 48 h. The confocal images depicted in Figure 5 showed that the untreated human cervical cancer cell line displayed the normal distribution of microtubules. However, cells treated with compounds **6c** and **6l** showed disrupted microtubule organization as seen in Figure 5, thus demonstrating the inhibition of tubulin polymerization. The density of microtubules was pronounced at the cell periphery with disorganized central networks and the standard CA4 also showed disrupted microtubule organization. This immunofluorescence study showed that the level of tubulin polymerization inhibition was comparable to that of CA4 for both **6c** and **6l**.

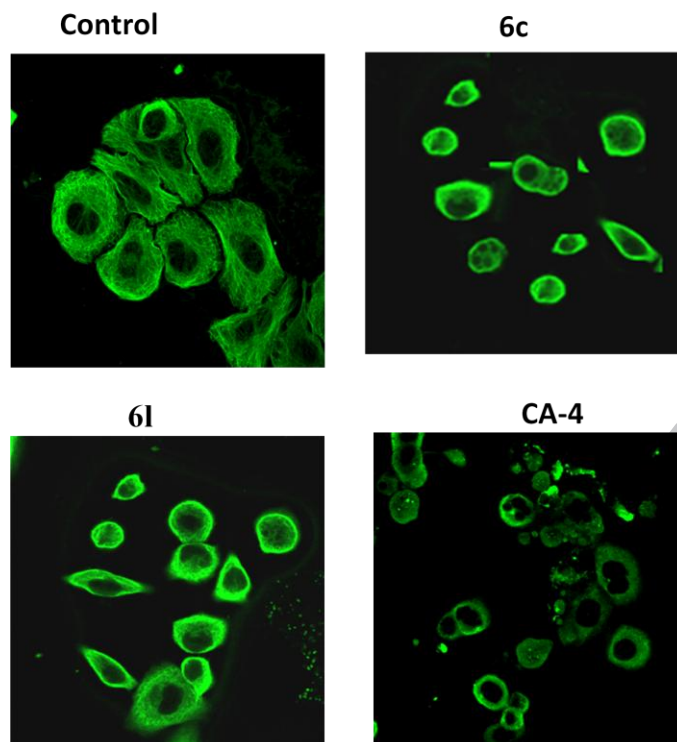


Figure 5. HeLa cells were treated with compounds **6c** and **6l** at 60 nM concentration for 48 h followed by staining with α -tubulin antibody. Microtubule organization was clearly observed by green colour tubulin network like structures in control cells and was found to be disrupted in cells treated with compounds **6c** and **6l**. CA4 was used as positive control. All pictures were taken in confocal microscopy equipped with 60X objective at scale bar 50 μ M.

Docking Studies

The above studies confirmed that both the potent mimics (**6c** and **6l**) disrupt the microtubule assembly by inhibition of tubulin polymerization as in case of CA4. We then proceeded to understand the possible mode of binding of by **6c** and **6l** at the colchicine site by performing a series of molecular docking analysis. These compounds were designed on the basis of the CA4 skeleton with modification of ring A and B in addition to ring replacement of the olefinic bridge. The lowest energy docking model resembles cochicine binding pose in the crystal structure (Figure 6A).³⁷ Pyridine ring mimics role of olefinic bond and CA4 mimics in cis-configuration.³⁸ The trimethoxyphenyl group in the benzothiazole mimic **6c** binds in hydrophobic region lined by residues Cys241 β , Leu242 β , Leu252 β , Leu255 β , Ala316 β , Val318 β , and Ile378 β . Specifically, R¹ methoxy fits in a hydrophobic pocket formed by Cys241 β , Leu242 β , Leu252 β and Leu255 β . Occupancy of this pocket seems to provide anchor point for the benzothiazole/benzimidazole

CA4 mimics. Activity of **5l/6c** further establishes that steric factor at R¹ is crucial for activity and trimethoxy group is not essential. Moderate activity of **5d-k** and **6g-k** (where R¹ is 'H' and R² is 'OMe/CF₃'), further strengthens this argument. This assumption agrees well with prior observations where modifications of trimethoxyphenyl moiety were well tolerated.³⁹ Further, the backbone carbonyl of Val238 β is close enough to R² position. It might be interesting to substitute a hydrogen-bond donor at R² position. 6-Methoxy group of benzimidazole moiety fits into a hydrophobic pocket formed by residues Val181 α , Thr314 β , Val315 β , Ala316 β and Met259 β . It is notable that benzimidazole rings fits in between Asn258 β and Lys352 β . Lys350 β (equivalent to Lys352 β) has been identified as a key residue by mutational studies.⁴⁰ Hence, addition of polar groups at position 4/5 of benzimidazole ring might improve potency by hydrogen-bonding with Lys352 side chain. The docked pose (Figure 6B) predicted along with the key interacting residues, also agrees well with the pharmacophore model developed based on diverse colchicine binding site inhibitors.⁴¹

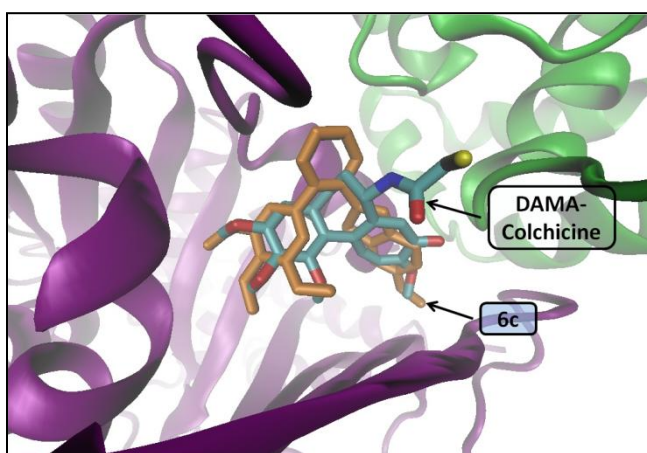


Fig 5A

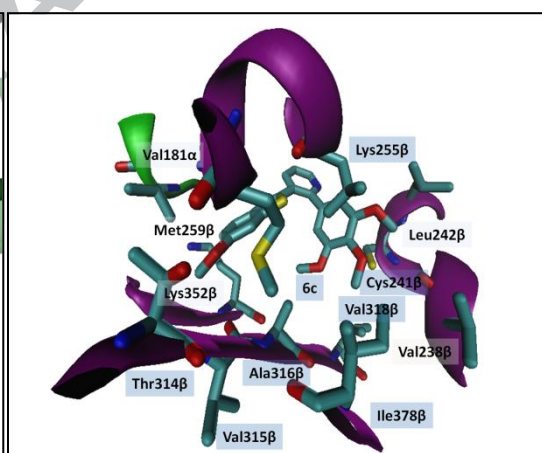


Fig 5B

Figure. 6. **A)** **6c** docked pose at the $\alpha\beta$ interface of tubulin. Residues within 3.5 Å of **6c** are shown. Backbone of residues is shown in cartoon representation. Backbone of α chain is shown in green and β chain in purple. **B)** Overlay of DAMA-Colchicine and **6c** docked pose is shown in orange and DAMA-Colchicine is colored by element. Backbone of α chain is shown in green and β chain in purple

Apoptosis Induction

Apoptosis is a tightly regulated process of destruction of undesirable cells during development or homeostasis in multicellular organisms. The induction of apoptosis is a well established strategy in the cancer drug discovery programs. In general, the microtubule perturbing agents are known

to arrest cell cycle in G2/M phase, which is followed by the loss of the mitochondrial transmembrane potential. This result in mitochondrial release of apoptogenic proteins leading to DNA fragmentation.⁴² In the present work, the apoptosis inducing ability of these *cis* restricted mimics of CA4 was studied which includes perturbation of mitochondrial membrane potential, activation of caspase cascade and subsequent DNA fragmentation.

Effect on Mitochondrial Membrane Depolarization

In order to quantify the loss of mitochondrial membrane potential using JC-1 stain, we also investigated the effects of **6c**, **6l** and CA4 on the JC-1 red/green ratio signals from isolated mitochondria. This was studied because the interference from the cytoplasm sometimes renders the interpretations of JC-1 signals in intact cells to be difficult.

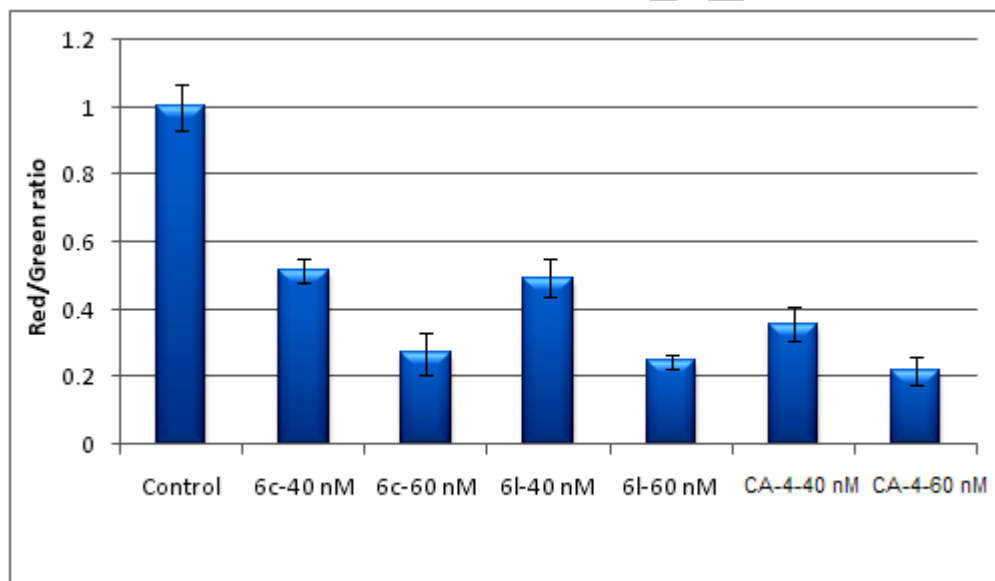


Figure 7. The emission ratio of the red and green fluorescence is shown. The first significant increase in ratio can be seen at 40 nM and 60 nM concentration of **6c** and **6l** respectively.

The use of isolated mitochondria largely removed the contributions from the cytoplasm redox-dependent signal transduction pathways. In this study, the mitochondria were challenged with **6c**, **6l** and CA4 in the presence of JC-1 stain. Results indicated that the JC-1 red/green ratio signal did not change in the control condition, indicating that the inner mitochondrial membrane potential was stable. Compounds **6c**, **6l** and CA4 were treated at 40 and 60 nM concentrations for 48 h. After incubation for 40 min, compounds **6c** and **6l** caused a slight decrease in the JC-1

red/green ratio signal when compared to control, whereas at 60 nM the compounds rapidly decreased the JC-1 red/green signal. The standard CA4 showed similar effect at both the concentration and **6l** exhibited comparable result to CA4 at higher concentration. The results demonstrated that **6c**, **6l** and CA4 rapidly decreased the JC-1 red/green ratio signal, corresponding to depolarization of the inner mitochondrial membrane potential (Figure 7).

In the present investigation we performed experiments to study the effect of **6c** and **6l** in triggering apoptosis in cancer cells.⁴³ It is well known that caspases play a crucial role in the induction of apoptosis and amongst the caspase cascade. Caspase-3 is one of the effector caspase which in turn is activated by caspase-9. Therefore to determine apoptosis inducing activity, conjugated caspase-3 and -9 substrates were employed and HeLa cells were treated with 40 nM and 60 nM concentrations of **6c** and **6l** along with CA4 as the positive control. The activation of caspase-9 and -3 were examined at two different time intervals as described in the procedure. Results indicate that **6l** exhibits superior caspase-3 activation than the standard CA4 with nearly 2 fold induction in both the caspases at 48 h (Figure 8).

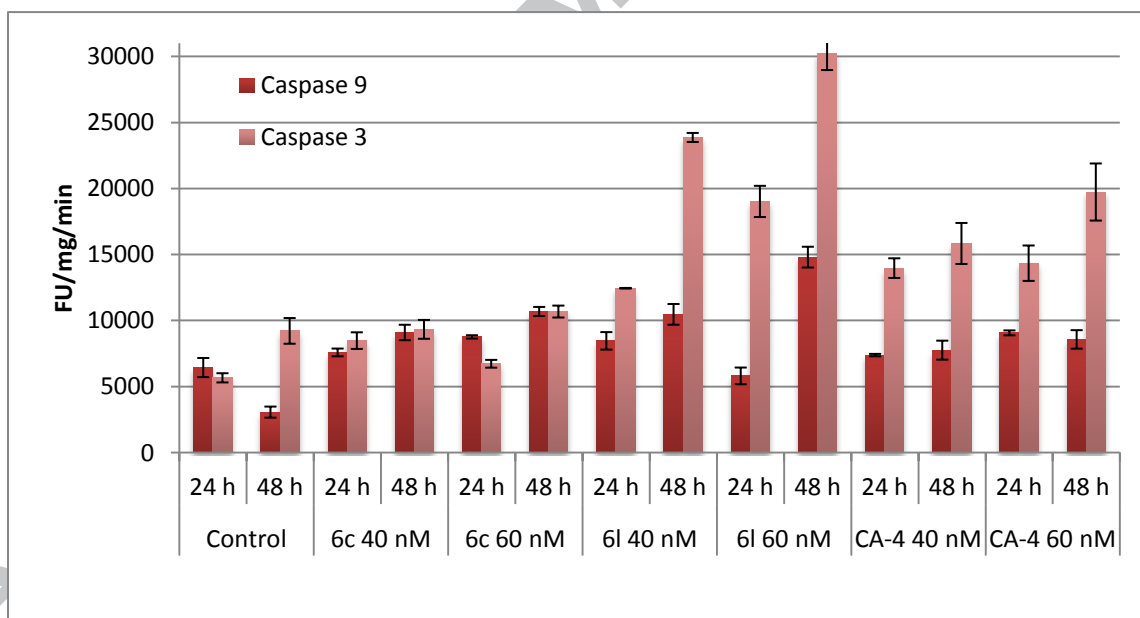


Figure 8. Effect of **6c** and **6l** at 40 nM and 60 nM concentrations on caspase-3 and caspase-9 in HeLa cells determined by fluorimetry at different time intervals, and CA4 is employed as the positive control.

In the present investigation, a series of *cis*-restricted benzimidazole (**5a-l**) and benzothiazole (**6a-n**) mimics of CA4 were designed and synthesized. On evaluation of cytotoxic activities against

selected human cancer cell lines, these mimics exhibited potent activity and the lead compounds like **6c** and **6l** displayed potent GI_{50} values in the range of $0.06 \pm 0.001 \mu M$ and $0.04 \pm 0.001 \mu M$, respectively against HeLa cells (human cervical cancer cell line). SAR studies suggested that importance of 3,4,5-trimethoxy substitution on ring A compared to 3,4-dimethoxy and 4-methoxy substitution pattern. The methoxy group on C-6 position of benzimidazole and benzothiazole moiety was essential for imparting potent antiproliferative activity and was crucial in these mimic with two electron withdrawing groups on ring A. In the case of mimic **6l** with trifluoromethyl on C-5 and chloro on C-2 position of ring A and methoxy group on C-6 position of benzothiazole moiety not only exhibited remarkable activity but was superior to CA4. FACS analysis demonstrated that the growth inhibitory effects of these CA4 mimics (**6c** and **6l**) were induced because of the arrest of cell cycle progression in G2/M phase comparable to CA4 in a concentration dependent manner. Tubulin polymerization assay showed that these mimics (**6c** and **6l**) are also potent inhibitors of tubulin polymerization and moreover the immunofluorescence studies demonstrated that they disrupt the microtubule organization. To understand the mode of binding, molecular docking studies were undertaken which demonstrated these mimics bind at the colchicine site of the tubulin. Further, **6c** and **6l** demonstrated loss of mitochondrial dysfunction which leads to two fold increase in induction of caspase-3 as well as caspase-9 compared to a standard at 40 nM and 60 nM concentrations. The SAR provided a useful insight that could be utilized in developing the lead compound **6l** as a potential antiproliferative agent. The mechanistic studies discussed are useful for the development of molecules based on such mimics as potential anticancer agents targeting tubulin.

Associated content

Supplementary data

Experimental procedures and spectra of 1H NMR, ^{13}C NMR, MS and HR-MS of compounds (**5a-l**) and (**6a-n**).

Author Information

Corresponding Author

* Phone: +91 40 27193157; Fax: +91-40-27193189. E-mail: ahmedkamal@iict.res.in.

Acknowledgments

M.A acknowledge CSIR-UGC, New Delhi and for the award of senior research fellowship. We also acknowledge CSIR for financial support under the 12th Five Year plan project “Affordable Cancer Therapeutics (ACT)” (CSC0301).

References and notes

1. Jordan, M. A.; Wilson, L. *Nat. Rev. Cancer*. **2004**, *4*, 253–265.
2. Hsieh, H. P.; Liou, J. P.; Lin, Y. T.; Mahindroo, N.; Chang, J. Y.; Yang, Y. N.; Chern, S. S.; Tan, U. K.; Chang, C. W.; Chen, T. W.; Lin, C. H.; Chang, Y. Y.; Wang, C. C. *Bioorg. Med. Chem. Lett.* **2003**, *13*, 101–105.
3. Belotti, D.; Vergani, V.; Drudis, T.; Borsotti, P.; Pitelli, M. R.; Viale, G.; Giavazzi, R.; Taraboletti, G. *Clin. Cancer Res.* **1996**, *2*, 1843–1849.
4. Mekhail, T. M.; Markman, M. *Expert Opin. Pharmacother.* **2002**, *3*, 755–766.
5. Rowinsky, E. K.; Donehower, R. C. *Pharmacol. Ther.* **1991**, *52*, 35–84.
6. Nam, N. H. *Curr. Med. Chem.* **2003**, *10*, 1697–1722.
7. Bhattacharyya, B.; Panda, D.; Gupta, S.; Banerjee, M. *Med. Res. Rev.* **2008**, *28*, 155–183.
8. Jordan, A.; Hadfield, J. A.; Lawrence, N. J.; McGown, A. T. *Med. Res. Rev.* **1998**, *18*, 259–296.
9. Dumontet, C.; Sikic, B. I. *J. Clin. Oncol.* **1999**, *17*, 1061–1070.
10. Tron, G. C.; Pirali, T.; Sorba, G.; Pagliai, F.; Busacca, S.; Genazzani, A. A. *J. Med. Chem.* **2006**, *49*, 3033–3044.
11. Siemann, D. W.; Chaplin, D. J.; Walicke, P. A. *Expert Opin. Invest. Drugs*. **2009**, *18*, 189–197.
12. Hori, K.; Saito, S. *Br. J. Cancer*. **2003**, *89*, 1334–1344.
13. Pettit, G. R.; Singh, S. B.; Hamel, E.; Lin, C. M.; Alberts, D. S.; Garcia-Kendall, D. *Experientia* **1989**, *45*, 209–211.
14. (a) Lin, C. M.; Ho, H. H.; Pettit, G. R.; Hamel, E. *Biochemistry* **1989**, *28*, 6984–6991. (b) Pettit, G. R.; Singh, S. B.; Boyd, M. R.; Hamel, E.; Pettit, R. K.; Schmidt, J. M.; Hogan, F. J. *Med. Chem.* **1995**, *38*, 1666–1672.

15. Demchuk, D. V.; Samet, A. V.; Chernysheva, N. B.; Ushkarov, V. I.; Stashina, G. A. ; Konyushkin, L. D.; Raihstat, M. M.; Firgang, S. I.; Philchenkov, A. A.; Zavelevich, M. P.; Kuiava, L. M.; Chekhun, V. F.; Blokhin, D. Y.; Kiselyov, A. S.; Semenova, M. N.; Semenov, V. V. *Bioorg. Med. Chem.* **2014**, *22*, 738-755.
16. Chen, H.; Li, Y.; Sheng, C.; Lv, Z.; Dong, G.; Wang, T.; Liu, J.; Zhang, M.; Li, L.; Tao Zhang, T.; Geng, D.; Niu, C.; Li, K. *J. Med. Chem.* **2013**, *56*, 685–699.
17. Cushman, M.; Nagarathnam, D.; Gopal, D.; He, H. M.; Lin, C. M. *J. Med. Chem.* **1992**, *35*, 2293-2306.
18. (a) Maya, A. B.; del Rey, B.; Lamamie de Clairac, R. P.; Caballero, E.; Barasoain, I. *Bioorg. Med. Chem. Lett.* **2000**, *10*, 2549-255.
19. Metzler, M.; Neumann, H. G. *Xenobiotica* **1977**, *7*, 117-132.
20. Simoni, D.; Grisolia, G.; Giannini, G.; Roberti, M.; Rondanin, R.; Piccagli, L.; Baruchello, R.; Rossi, M.; Romagnoli, R.; Invidiata, F. P.; Grimaudo, S.; Jung, M. K.; Hamel, E.; Gebbia, N.; Crosta, L.; Abbadessa, V.; Cristina, A. D.; Dusonchet, L.; Meli, M.; Tolomeo, M. *J. Med. Chem.* **2005**, *48*, 723-736.
21. Zhang, Q.; Peng, Y.; Wang, X. I.; Keenan, S. M.; Arora, S.; Welsh, W. J. *J. Med. Chem.* **2007**, *50*, 749-754.
22. Romagnoli, R.; Baraldi, P. G.; Salvador, M. K.; Preti, D.; Tabrizi, M. G.; Brancale, A.; Fu, X. H.; Li, J.; Zhang, S. Z.; Hamel, E.; Bortolozzi, R.; Basso, G.; Viola, G. *J. Med. Chem.* **2012**, *55*, 475–488.
23. <http://clinicaltrials.gov/>
24. Yokoi, A.; Kuromitsu, J.; Kawai, T.; Nagasu, T.; Sugi, N. H.; Yoshimatsu, K.; Yoshino, H.; Owa, T. *Mol. Cancer Ther.* **2002**, *1*, 275-286.
25. Yoshimatsu, K.; Yamaguchi, A.; Yoshino, H.; Koyanagi, N.; Kitoh, K. *Cancer Res.* **1997**, *57*, 3208-3213.
26. Kavallaris, M.; Verrills, N. M.; Hill, B. T. *Drug Resist Updat.* **2001**, *4*, 392-401.

27. Mauer, A. M.; Cohen, E. E.; Ma, P. C.; Kozloff, M. F.; Schwartzberg, L.; Coates, A. I.; Qian, J.; Hagey, A. E.; Gordon, G. B. *J. Thorac Oncol.* **2008**, *3*, 631-636.
28. Liu, Z.; Zhou, Z.; Tian, W.; Fan, X.; Xue, D.; Yu, L.; Yu, Q.; Long, Y. Q. *Chem. Med. Chem.* **2012**, *7*, 680-693.
29. Kamal, A.; Sreekanth, Y. V. V.; Shaik, T. B.; Khan, M. N. A.; Ashraf, Md.; Reddy, M. K.; Kumar, K. A.; Kalivendi, S. V. *Med. Chem. Commun.* **2011**, *11*, 819.
30. Kamal, A.; Mallareddy, A.; Suresh, P.; Shaik, T. B.; Lakshma Nayak, V.; Kishor, C.; Shetti, R. V.; Rao, N. S.; Tamboli, J. R.; Ramakrishna, S.; Addlagatta, A. *Bioorg. Med. Chem.* **2012**, *20*, 3480-3492.
31. Kamal, A.; Ashraf, Md.; Vardhan, M. V. P. S. V.; Faazil, S.; Lakshma Nayak, V. *Bioorg. Med. Chem. Lett.* **2013**, *24*, 147-151.
32. Tishler, R. T.; Lamppu, D. M.; Park, S.; Price, B. D. *Cancer Research* **1995**, *55*, 6021-6025.
33. Kamal, A.; Mallareddy, A.; Ramaiah, M. J.; Pushpavalli, S.N.; Suresh, P.; Kishor, C.; Murty, J. N.; Rao, N. S.; Ghosh, S.; Addlagatta, A.; Pal-Bhadra, M. *Eur. J. Med. Chem.* **2012**, *56*, 166-178.
34. Kamal, A.; Srikanth, Y. V. V.; Khan, M. N. A.; Ashraf, M.; Reddy, M. K.; Sultana, F.; Kaur, T.; Chashoo, G.; Suri, N.; Sehar, I.; Wani, Z. A.; Saxena, A.; Sharma, P.R.; Bhushan, S.; Mondhe, D. M.; Saxena, A. K.; *Bioorg. Med. Chem.* **2011**, *11*, 7136.
35. Theeramunkong, S.; Caldarelli, A.; Massarotti, A.; Aprile, S.; Caprioglio, D.; Zaninetti, R.; Teruggi, A.; Pirali, T.; Grosa, G.; Tron, G. C.; Genazzani, A. A. *J. Med. Chem.* **2011**, *54*, 4977-4986.
36. Vichai, V.; Kirtikara, K. *Nat. Protoc.* **2006**, *1*, 1112-1116.
37. Ravelli, R. B.; Gigant, B.; Curmi, P. A.; Jourdain, I.; Lachkar, S.; Sobel, A.; Knossow, M. *Nature* **2004**, *428*, 198-202.
38. Timothy J. Snape, Katherine Karakoul, FarzanaRowther and Tracy Warr, RSC Advances, **2012**, *2*, 7557-7560
39. Tron, G. C.; Pirali, T.; Sorba, G.; Pagliai, F.; Busacca, S.; Genazzani, A. A. *J. Med. Chem.* **2006**, *49*, 3033-3044.
40. Xuequn Helen Hua *Cancer Res.* **2001**, *61*, 7248-7254

41. Yan Lu, Jianjun Chen, Min Xiao, Wei Li, and Duane D. Mille, *Pharm Res.* **2012** Nov; 29(11): 2943-2971
42. Kawabata, Y.; Hirokawa, M.; Kitabayashi, A.; Horiuchi, T.; Kuroki, J.; Miura, A. B. *Blood.* **1999**, 94, 3523-3530.
43. Kumar, S. *Cell Death Differ.* **2007**, 14, 32-43.
44. Bonne, D.; Heusele, C.; Simon, C. Pantaloni, D. *J. Biol. Chem.* **1985**, 260, 2819-2825.
45. Huber, K.; Patel, P.; Zhang, L.; Evans, H.; Westwell, A. D.; Fischer, P. M.; Chan S. Martin, S. *Mol. Cancer Ther.* **2008**, 7, 143-151.
46. Smiley, S. T.; Reers, M.; Hartshorn, C. M.; Lin, M.; Chen, A.; Smith, T. W.; Steele, G. D. Jr.; Chen, L. B. *Proc. Natl. Acad. Sci. U S A.* **1991**, 88, 3671-3675.
47. Morris, G. M.; Huey, R.; Lindstrom, W.; Sanner, M. F.; Belew, R. K.; Goodsell, D. S.; Olson, A. J. *J. Comput. Chem.* **2009**, 30, 2785-2791.
48. (a) Seel, K. *J. Volunt. Adm.* **1996**, 14, 33-38. (b) Humphrey, W.; Dalke, A.; Schulten, K. *J Mol Graph.* **1996**, 14, 33-38.

Graphical Abstract

Design and synthesis of *cis*-restricted benzimidazole and benzothiazole mimics of combretastatin A-4 as antimitotic agents with apoptosis inducing ability

Md. Ashraf, Thokhir B Shaik, M Shaheer Malik, Riyaz Syed, Prema L Mallipeddi, M V P S

Vishnu Vardhan, Ahmed Kamal*

